Supporting Information

Dillman et al. 10.1073/pnas.1211436109

SI Materials and Methods

Nematodes. *Heterorhabditis bacteriophora* was from the inbred strain M31e (1–3). *Steinernema carpocapsae* was from the inbred strain ALL (3, 4). *Caenorhabditis elegans* was the wild isolate CB4856 ("Hawaii"). *Oscheius carolinensis* was the YEW strain (5). *Steinernema glaseri* was from the inbred NC strain (6). *Steinernema scapterisci* was inbred from the FL strain (7). *Steinernema riobrave* was inbred from the TX strain (8).

Nematode Culturing. All nematodes were cultured as previously described (3). Briefly, five last-instar *Galleria mellonella* larvae (American Cricket Ranch) were placed in a 5-cm Petri dish with 55-mm Whatman 1 filter paper acting as a pseudosoil substrate in the bottom of the dish. Water (≤250 μL) in which 500–1,000 infective juveniles (IJs) were suspended was distributed evenly on the filter paper. After 7–10 d the insect cadavers were placed on White traps (9). *Steinernema glaseri* was placed onto a modified White trap containing plaster of Paris as previously described (10). Emerging IJs were harvested and rinsed three times with water. *S. scapterisci* also was cultured by infecting house crickets and mole crickets using similar techniques. IJs were stored at either room temperature or 15 °C and were tested within 2 mo of emergence. *C. elegans* was cultured on nematode growth media plates seeded with *Escherichia coli* OP50 according to standard methods (11), and dauer larvae were collected from the lids of plates from which the nematodes had exhausted their bacterial food supply (i.e., "starved plates").

Nematode Phylogeny. Small subunit ribosomal DNA (SSU rDNA) sequences for the large phylogenetic analysis were obtained from GenBank for all taxa included in the present study (accession numbers: AJ920356, EU086375, AF036593, AY268117, U81584, AF083007, AF279916, AF036604, AY284620, AY284621, AY284671, U94367, AF036588, U61761, AF036600, U60231, EU344798, X87984, AF036589, AF519234, AJ920348, FJ547240, AJ417024, U81581, and AF036639). A total of 23 nematode species and two outgroup taxa (a priapulid and a nematomorph) were used in the analyses for Fig. S1*A*. Sequences were aligned using ProAlign (12) with 1,500 Mb of memory allotted and bandwidth set to 1,500 Mb with Hidden Markov Model (HMM) parameters being estimated from the data. We excluded characters aligned with posterior probability values under 60%, resulting in 1,330 aligned characters for subsequent analysis. The TIM2+I+G model was selected as the best-fit model of substitution for all analyses using the AIC and BIC model selection criteria in the program jModelTest (13, 14). Maximum likelihood (ML) and bootstrap (1,000 replicates) analyses were carried out in PhyML 3.0 (15) using the parameters for base frequencies, substitution rate matrix, proportion of invariable sites, number of substitution categories, and shape distribution parameter determined as the best-fit by jModelTest [freqA = 0.2618, freqC = 0.1850, freqG = 0.2443, freqT = 0.3089, Ra(AC) = 1.4966, Rb(AG) = 2.4339, Rc(AT) = 1.4966, Rd(CG) = 1.0000, Re(CT) = 3.7721, Rf(GT) = 1.0000, p-inv = 0.1150, and gamma shape = 0.5290]. Bayesian analysis was carried out using MrBayes 3.1.2 (16). The number of substitution categories and shape was based on the parameters determined by jModelTest (as above). The parameters for base frequencies, relative rates, substitution rate matrix, and proportion of invariant sites were allowed to vary throughout the analysis. The parameters shape, statefreq, and revmat were unlinked to allow more flexibility in searching tree space. Trees were sampled every 1,000 generations. The burn-in value was set to 2,000 trees. The total number of generations was set to 8 million. Four parallel chains (one cold and three heated) were used. A majority-rule consensus tree was reconstructed after discarding the burn-in.

For the four *Steinernema* species phylogeny (Fig. S1*B*), large subunit ribosomal DNA (LSU rDNA) sequences were obtained from GenBank (AF331908, AF331898, AF331893, AF331900, and DQ145647). Sequences were aligned using ProAlign (12) with 1,050 Mb of memory allotted and bandwidth set to 1,000 Mb with HMM model parameters being estimated from the data. We excluded characters aligned with posterior probability values under 60%, resulting in 883 aligned characters for subsequent analysis. The TIM3+G model was selected as the best-fit model of substitution for all analyses using both the AIC and BIC model selection criteria in the program jModelTest (13, 14). ML and bootstrap (1,000 replicates) analyses were carried out in PhyML 3.0 (15) using the parameters for substitution rate matrix, proportion of invariable sites, number of substitution categories, and shape distribution parameter determined as the best-fit by jModelTest [Ra(AC) = 0.3610, Rb(AG) = 1.1251, Rc(AT) = 1.0, Rd(CG) = 0.3610, Re(CT) = 3.9194, Rf(GT) = 1.0000, gamma shape = 0.5.650]. Base frequencies were estimated empirically, and the p-invar parameter was optimized from the data. Bayesian analysis was carried out using MrBayes 3.1.2 (16). The number of substitution categories was based on the parameters determined by jModelTest (as above). Other parameters, such as base frequency, relative rates, substitution rate matrix, and proportion of invariant sites, were allowed to vary throughout the analysis. The parameters shape, statefreq, and revmat were unlinked to allow more flexibility in searching tree space. Trees were sampled every 1,000 generations. The burn-in value was set to 2,000 trees. The total number of generations was set to 8 million. Four parallel chains (one cold and three heated) were used. A majority-rule consensus tree was reconstructed after discarding the burn-in.

Collection of Potential Hosts. Mole crickets, earwigs, flatheaded borers, pillbugs, and slugs were collected from their natural habitats in the greater Los Angeles area and tested within a few weeks of collection. The majority of the earwigs, flatheaded borers, pillbugs, and slugs were collected from the campus of the California Institute of Technology (Fig. S2). Mole crickets were collected from the Rio Hondo golf course in Downey, CA. Waxworms and house crickets were purchased commercially from American Cricket Ranch or Petco. For potential hosts collected from natural habitats, species identities were confirmed by analysis of 18S ribosomal DNA sequence, knowledge of habitat distributions in Southern California, and analysis of diagnostic external morphological features.

Chemotaxis Assays. Host, CO_2, and odorant chemotaxis assays were performed as previously described (3). Briefly, assays were performed on standard chemotaxis assay plates (17). Scoring regions consisted circles 2 cm in diameter along the edge of each side of the plate, with the center of the circle 1 cm from the edge of the plate. For host chemotaxis assays, live hosts (one animal in the case of mole crickets, and four to six animals for all other hosts) were placed into a 50-mL gastight syringe (Hamilton), and a control syringe was filled with room air. Syringes were depressed at a rate of 0.5 mL/min using a syringe pump (Harvard Apparatus). Host air was delivered to one side of the assay plate, and room air was delivered to the other side of the assay plate through holes drilled into the plate lids directly above the centers

of the scoring regions. For CO_2 chemotaxis assays, gastight syringes were filled with either a certified CO_2 mixture containing the test concentration of CO_2, 10% O_2, and the balance N_2 or a control air mixture containing 10% O_2 and 90% N_2. For odorant chemotaxis assays, 1 μL of 1 M sodium azide was placed in the center of each scoring region as an anesthetic. Then 5 μL of odorant (Sigma-Aldrich or Fisher) was placed in the center of one scoring region, and 5 μL of a control (paraffin oil, dH_2O, or ethanol) was placed in the center of the other scoring region. For all assays, ∼2 μL of worm pellet containing ∼50–150 nematodes was placed in the center of the assay plate. Assay plates were left undisturbed on a vibration-reducing platform and were scored after 1 h (for host and CO_2 chemotaxis assays) or after 3 h (for odorant assays). If at least three worms moved into the scoring regions, a chemotaxis index (C.I.) was calculated as C.I. = (number of worms at CO_2 − number of worms at air)/(number of worms at CO_2 + number of worms at air). For the soda lime host chemotaxis assay, gas mixtures were passed through a 6-in column containing 2–5 mm soda lime pellets (72073; Sigma-Aldrich) before entering the assay plate as described previously (3). Solid odorants were dissolved as follows: 3-hydroxy-2-butanone and dimethyl sulfone, 1 g in 4 mL dH_2O; 4-methylphenol and p-dichlorobenzene, 0.1 g in 5 mL paraffin oil; and p-benzoquinone, 0.1 g in 5 mL ethanol.

For the mixture assay shown in Fig. 7*A*, the control assay (left bar) had 5 μL of an odorant mix containing 10^{-1} dilutions of p-dichlorobenzene, hexanal, and γ-terpinene on one side of the chemotaxis plate and 5 μL of paraffin oil control on the other side. The experimental assay (right bar) had 5 μL of odorant mix containing 10^{-1} dilutions of p-dichlorobenzene, hexanal, and γ-terpinene on one side of the chemotaxis plate and 5 μL of odorant mix containing 10^{-1} dilutions of p-dichlorobenzene, hexanal, γ-terpinene, and 3-hydroxy-2-butanone on the other side. The soil assay shown in Fig. 7*B* used a modified version of the CO_2 and host chemotaxis assays. For the control assay (left bar), one syringe contained 3 g of soil (collected from the sampling site shown in Fig. S2), and the other syringe contained air. For the experimental assay (right bar), one syringe contained 3 g of soil plus 5 μL paraffin oil on a small piece of filter paper and the other syringe contained 3 g of soil plus 5 μL of 4-methylphenol (dissolved as described above) on a small piece of filter paper.

Jumping Assay. Jumping assays were performed as previously described (3). Briefly, 100 IJs suspended in 200 μL water were distributed evenly onto 55-mm Whatman 1 filter paper on the bottom of a 5-cm Petri dish. For host jumping assays, a single live host was placed into a 10-mL gastight syringe (Hamilton), and a control syringe was filled with room air. For CO_2 jumping assays, syringes were filled with either a certified CO_2 mixture or air control as described above. For odorant jumping assays, a small piece of filter paper containing 5 μL of undiluted odorant was placed inside a plastic syringe (Beckton Dickinson) syringe. The needle from the syringe was inserted through a 1.25-mm hole in the side of the dish so that the tip of the needle was within ∼2 mm of a standing IJ. A small puff of air from the syringe (∼0.5 mL volume) then was administered directly at the IJ, and a jumping response was scored if the IJ jumped within 8 s. Approximately 20 IJs were tested from the same arena. Then a normalized jumping index (J.I.) that ranged from −1 to +1 was calculated. For stimuli that evoked higher levels of jumping than the control, the J.I. and SEM were calculated as J.I. = (fraction jumped to stimulus − fraction jumped to control)/(1 − fraction jumped to control) and SEM = $\sqrt{[(\text{SEM for stimulus})^2 - (\text{SEM for control})^2]}/(1 - \text{fraction jumped to control})$. For stimuli that evoked lower levels of jumping than the control, the J.I. and SEM were calculated as J.I. = (fraction jumped to stimulus − fraction jumped to control)/(fraction jumped to control) and SEM = $\sqrt{[(\text{SEM for stimulus})^2 - (\text{SEM for control})^2]}/(\text{fraction jumped}$ to control). For soda lime host jumping assays, the assay setup was as described above, but gas mixtures were passed through a 2-in column of Nalgene (8050-0250) FTP 3/16-in o.d. tubing containing 2–5 mm soda lime pellets (72073; Sigma-Aldrich) before entering the assay arena. The column was held between two female-ended Swagelok compression fittings. To attach the column to the syringe and needle securely, the Swagelok fittings were filled with a male (on the needle end) and female (on the syringe end) biomedical Luer fitting.

Virulence Assay. Individual hosts, except for mole crickets, were placed into 5-cm Petri dishes (mole crickets were placed in small glass baby food jars with an air hole drilled into the lid) containing 55-mm Whatman 1 filter paper at the bottom. Then 100 IJs suspended in 200 μL water were distributed evenly onto the filter paper. Hosts were exposed to IJs for 48 h at room temperature, and host survival was then scored by response to gentle prodding. To assay entomopathogenic nematode (EPN) growth and reproduction in host cadavers, the cadavers were dissected at 5 d postexposure and scored for the presence of either adult EPNs only (growth but not reproduction) or adults and young larvae (growth and reproduction). To assay emergence from host cadavers, cadavers were placed onto standard White traps (9) at 10 d postexposure (all hosts except house crickets) or 5 d postexposure (house crickets) and scored for the presence of IJs in the trap at 20 d postexposure. For potential hosts that desiccate easily (mole crickets, house crickets, pillbugs, and slugs), 200 μL water was added to the filter paper each day to prevent desiccation.

Identification of Host-Derived Odorants by Thermal Desorption-Gas Chromatography-Mass Spectrometry and Solid-Phase Microextraction-Gas Chromatography-Mass Spectrometry. Thermal desorption-gas chromatography-mass spectrometry (TD-GC-MS) was performed as previously described (3). TD-GC-MS data for waxworms and house crickets are from Hallem et al. (3). Both the collection of volatile organic compounds (VOCs) and subsequent solid-phase microextraction (SPME) analysis were modified from Villaverde et al. (18). Briefly, VOCs were collected for SPME analysis by placing insects into 10-mL glass vials sealed with a Teflon septum (27529; Supleco). Larger and potentially cannibalistic insects (mole crickets and house crickets) were placed individually into sampling vials; smaller species (waxworms, flat-headed borers, pillbugs, and earwigs) were sampled with four individuals per sampling vial. Experiments were done in pairs and replicated three times, with an empty control sampling vial being run each time. Clean, sterile vials were used each time. After 12 h, secreted volatiles were sampled from the head space, corresponding to the gaseous phase in contact with the insect sample. VOCs were sampled for 15 min using carboxen/polydimethylsiloxane fiber (75-mm film thickness) (504831; Supelco). Selection of fibers was based on manufacturer's recommendations for sampling volatiles of low to intermediate polarity and from data reported by Villaverde et al. (18). Fibers were preconditioned in accordance with the manufacturer's instructions. Quantitative analysis was performed using a Hewlett Packard 6890 GC–5973 MS gas chromatograph-mass spectrometer (Agilent Technologies) using a nonpolar DB-5 capillary column (30 m × 0.25 mm, 0.25-μm film thickness) (Agilent Technologies). The injector was operated in the splitless mode at 250 °C, and the oven temperature was programmed (40 °C for 3 min, 5 °C/min to 80 °C, 20 °C/min to 150 °C, and 30 °C/min to 250 °C, with a holding time of 10 min at the final temperature). The transfer line temperature was set at 280 °C, and the ion source was held at 250 °C. VOC identification was performed by capillary gas chromatography (CGC)-MS analysis with an Eclipse 4660 purge and trap sampler with chromatographic conditions similar to the CGC; the ion source was set at 200 °C and the transfer line at 275 °C. VOCs were tentatively identified by interpretation of their mass spectral

fragmentation. Data were analyzed with both Chemstation and Masshunter software. Mass spectra also were compared with data from the Wiley library (275,000 spectra) of electron impact mass spectra. Only compounds that were found in multiple traces (≥2) with a relative abundance ≥20,000, that were not present in the control traces, and that had library matches of ≥95% were considered in this study.

Data Analysis. Statistical analysis was performed using GraphPad Instat, GraphPad Prism, or PAST (19). Two-factor ANOVAs with Bonferroni posttests were used to compare the responses of the different EPNs to the different hosts or host-derived odorants. *P* values from the ANOVAs (factor 1, factor 2, and the interaction between the factors) are given in the figure legends; *P* values from the posttests are given in the SI datasets. For example, when examining the responses of the different EPNs to the different hosts, we show that EPNs respond differently to different hosts ($P < 0.0001$ for factor one), that different hosts evoke different overall responses from EPNs ($P < 0.0001$ for factor two), and that different EPNs show different odor–response profiles ($P < 0.0001$ for the interaction). Heatmaps were generated using Heatmap Builder (20).

1. Hallem EA, Rengarajan M, Ciche TA, Sternberg PW (2007) Nematodes, bacteria, and flies: A tripartite model for nematode parasitism. *Curr Biol* 17:898–904.
2. Ciche TA, Kim KS, Kaufmann-Daszczuk B, Nguyen KC, Hall DH (2008) Cell invasion and matricide during *Photorhabdus luminescens* transmission by *Heterorhabditis bacteriophora* nematodes. *Appl Environ Microbiol* 74:2275–2287.
3. Hallem EA, et al. (2011) A sensory code for host seeking in parasitic nematodes. *Curr Biol* 21:377–383.
4. Bilgrami AL, Gauger R, Shapiro-Ilan DI, Adams BJ (2006) Source of trait deterioration in entomopathogenic nematodes *Heterorhabditis bacteriophora* and *Steinernema carpocapsae* during *in vivo* culture. *Nematology* 8(3):397–409.
5. Ye W, Torres-Barragan T, Cardoza YJ (2010) *Oscheius carolinensis* n. Sp. (Nematoda: Rhabditidae), a potential entomopathogenic nematode from vermicompost. *Nematol* 12(1):121–135.
6. Li XY, Cowles EA, Cowles RS, Gaugler R, Cox-Foster DL (2009) Characterization of immunosuppressive surface coat proteins from *Steinernema glaseri* that selectively kill blood cells in susceptible hosts. *Mol Biochem Parasitol* 165:162–169.
7. Nguyen KB, Smart GC (1991) Pathogenicity of *Steinernema scapterisci* to selected invertebrates. *J Nematol* 23(1):7–11.
8. Canhilal R, Reid W, Kutuk H, El-Bouhssini M (2007) Susceptibility of sunn pest, *Eurygaster integriceps* Puton (Hemiptera: Scutelleridae), to various entomopathogenic nematodes (Rhabditida: Steinernematidae and Heterorhabditidae). *J Agr Urban Entomol* 24(1):19–26.
9. White GF (1927) A method for obtaining infective nematode larvae from cultures. *Science* 66(1709):302–303.
10. Kaya HK, Stock SP (1997) Techniques in insect nematology. *Manual of Techniques in Insect Pathology*, ed Lacey LA (Academic Press, San Diego), pp 281–324.
11. Brenner S (1974) The genetics of *Caenorhabditis elegans*. *Genetics* 77:71–94.
12. Löytynoja A, Milinkovitch MC (2003) A hidden Markov model for progressive multiple alignment. *Bioinformatics* 19:1505–1513.
13. Posada D (2009) Selection of models of DNA evolution with jModelTest. *Methods Mol Biol* 537:93–112.
14. Guindon S, Gascuel O (2003) A simple, fast, and accurate algorithm to estimate large phylogenies by maximum likelihood. *Syst Biol* 52:696–704.
15. Guindon S, et al. (2010) New algorithms and methods to estimate maximum-likelihood phylogenies: Assessing the performance of PhyML 3.0. *Syst Biol* 59:307–321.
16. Huelsenbeck JP, Ronquist F (2001) MRBAYES: Bayesian inference of phylogenetic trees. *Bioinformatics* 17:754–755.
17. Bargmann CI, Hartwieg E, Horvitz HR (1993) Odorant-selective genes and neurons mediate olfaction in *C. elegans*. *Cell* 74:515–527.
18. Villaverde ML, Juarez MP, Mijailovsky S (2007) Detection of *Tribolium castaneum* (herbst) volatile defensive secrections by solid phase microextraction-capillary gas chromatrophy (SPME-CGC). *J Stored Prod Res* 43:540–545.
19. Hammer Ø, Harper DAT, Ryan PD (2001) PAST: Paleontological statistics software package for education and data analysis. *Palaeontol Electronica* 4(1): 9 pp.
20. King JY, et al. (2005) Pathway analysis of coronary atherosclerosis. *Physiol Genomics* 23:103–118.

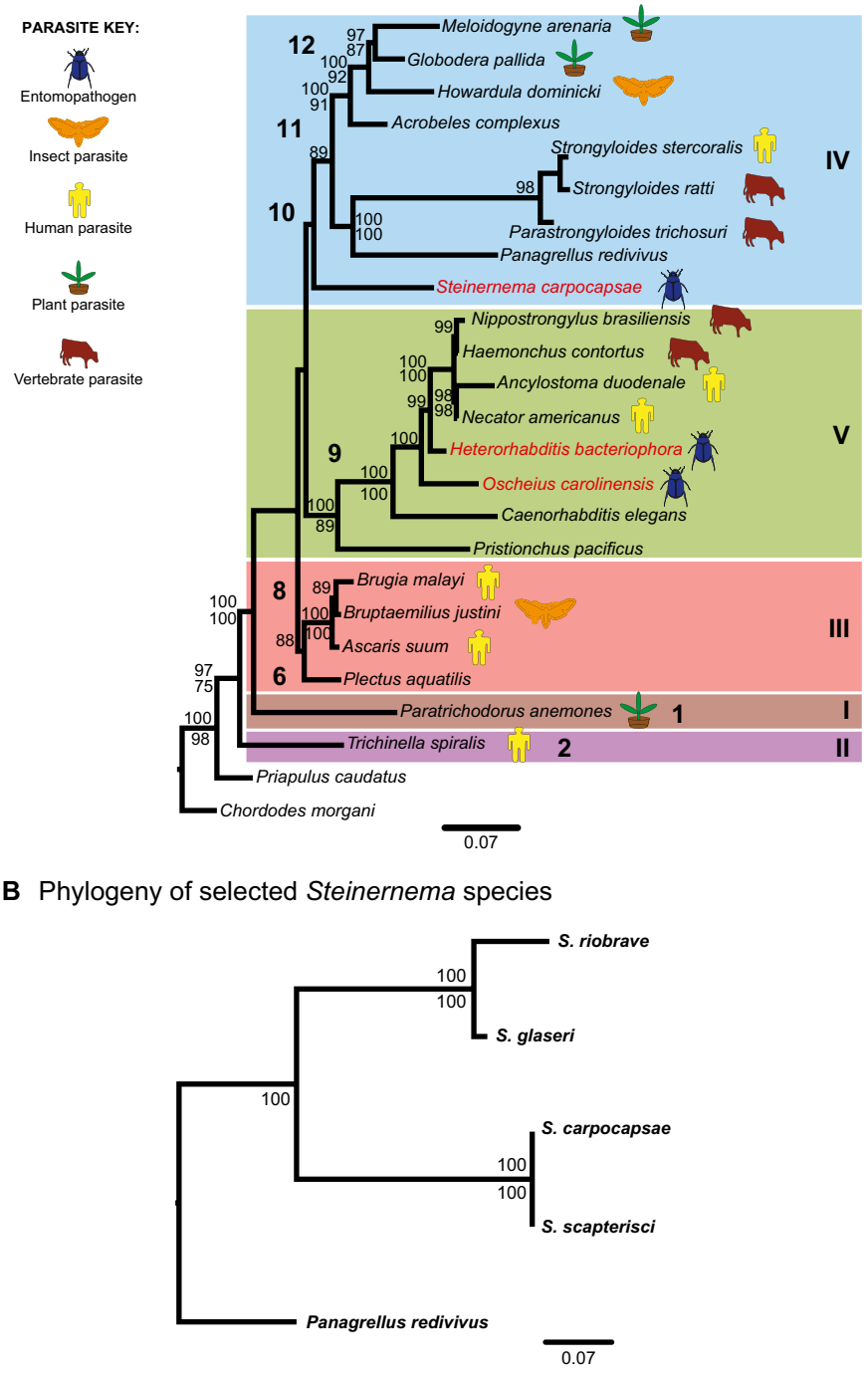

Fig. S1. Phylogeny of selected nematodes. (*A*) Phylogenetic relationships among free-living and parasitic nematodes. Relationships are based on ML and Bayesian analyses of nearly complete SSU sequences. Values above each branch represent Bayesian posterior probabilities; ML bootstrap indices appear below each branch. Values lower than 75 are not reported. The two analyses produced concordant tree topologies. Nematode clades 1–12 are after Holterman et al. (1); clades after Blaxter et al (2) are indicated by roman numerals and colored boxes. For parasitic species, hosts are indicated by colored icons. *Priapulus* (a priapulid) and *Chordodes* (a nematomorph) were defined as outgroups. (*B*) Phylogeny of selected *Steinernema* species. Relationships are based on ML and Bayesian analysis of the LSU rDNA. Values above each branch represent Bayesian posterior probabilities; ML bootstrap indices appear below each branch. Values <75 are not reported. The two analyses produced concordant tree topologies. The tree was rooted with the free-living nematode *Panagrellus redivivus* as the outgroup species.

1. Holterman M, et al. (2006) Phylum-wide analysis of SSU rDNA reveals deep phylogenetic relationships among nematodes and accelerated evolution toward crown Clades. *Mol Biol Evol* 23:1792–1800.
2. Blaxter ML, et al. (1998) A molecular evolutionary framework for the phylum Nematoda. *Nature* 392:71–75.

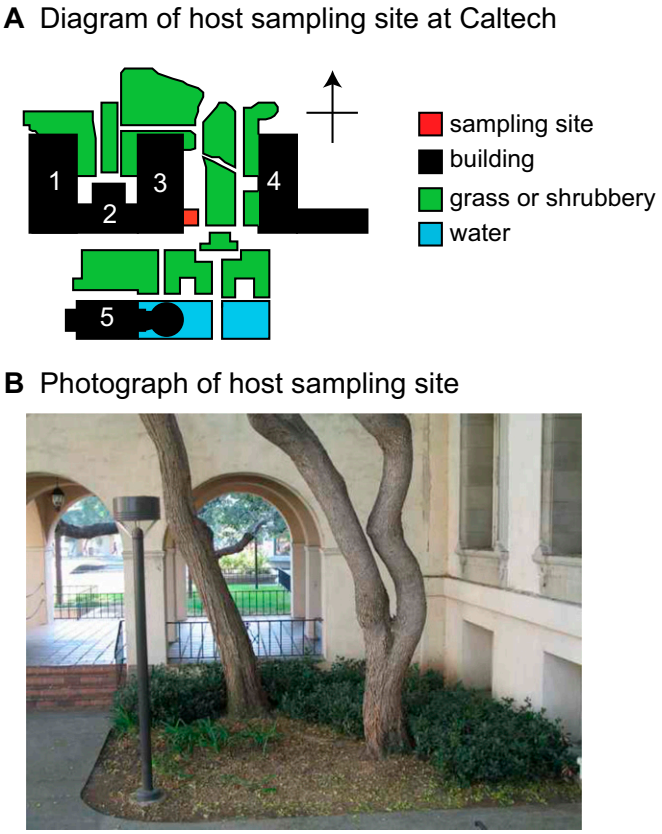

Fig. S2. Sampling site from which the majority of potential hosts were collected. (*A*) Diagram of the sampling site at the California Institute of Technology. (*B*) Photograph of the same sampling site. The sampling site is the small, shady grass plot visible in the foreground. Earwigs, pillbugs, and slugs were collected from the upper layers of moist soil in the vicinity of a leaky sprinkler. Flatheaded borers were collected from inside the wood of nearby rose bushes.

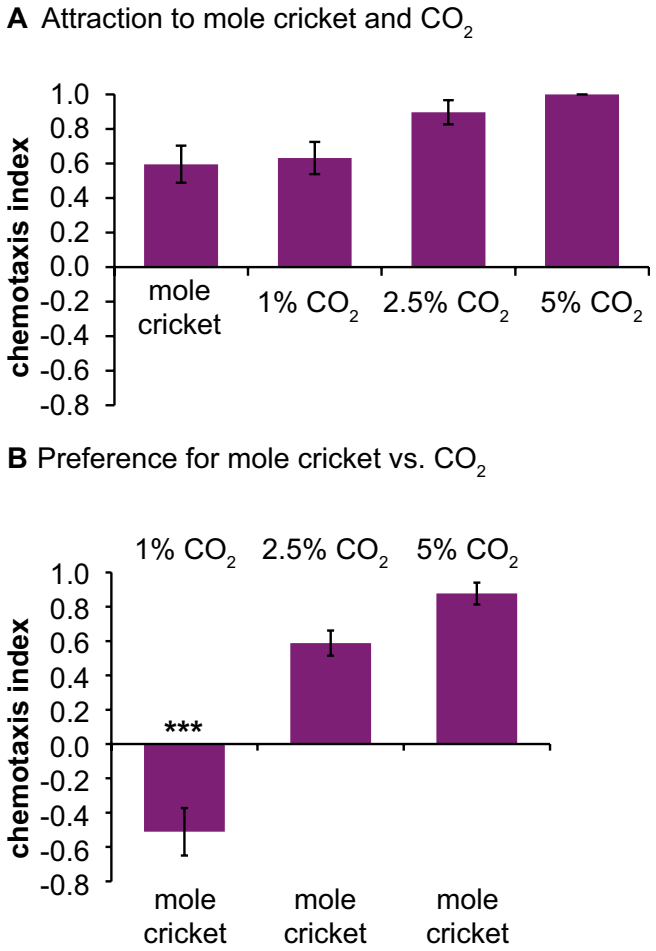

Fig. S3. Preference of *S. carpocapsae* IJs for mole cricket odor vs. CO_2. (*A*) Responses of *S. carpocapsae* IJs to volatiles from an individual mole cricket and to different concentrations of CO_2 in a chemotaxis assay. Data are from Figs. 1*B* and 3*A*. (*B*) Responses of *S. carpocapsae* IJs to volatiles from an individual mole cricket vs. different concentrations of CO_2 in a competition chemotaxis assay. A positive C.I. indicates attraction to CO_2; a negative C.I. indicates attraction to mole cricket odor. n = 3–9 trials for each condition. The response to mole cricket odor when tested against an air control was not significantly different from the response to mole cricket odor when tested against 1% CO_2 (unpaired t test). The response to 1% CO_2 when tested against an air control was significantly different from the response to 1% CO_2 when tested against mole cricket odor (***, $P < 0.001$); however, responses to 2.5% CO_2 and 5% CO_2 when tested against an air control vs. mole cricket odor were not significantly different (two-factor repeated measures ANOVA).

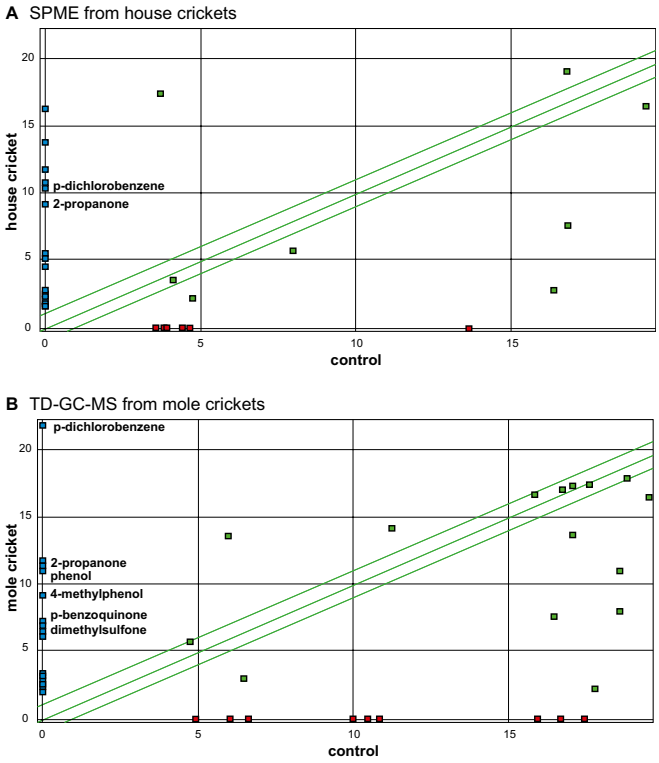

Fig. S4. Identification of host-derived odorants by GC-MS. (*A*) A representative trace showing SPME-GC-MS data obtained from live house crickets. (*B*) A representative trace showing TD-GC-MS data obtained from live mole crickets. For both graphs, the *x*-axis indicates the relative abundance in control air, and the *y*-axis indicates relative abundance in host air. Odorants found exclusively in host air are indicated in blue, odorants found exclusively in control air are indicated in red, and odorants found in both host air and control air are indicated in green. Of the odorants found exclusively in host air, only those identified in multiple experimental replicates at a relative abundance of ≥20,000 and with a library match of ≥95% confidence are labeled, with the exception of p-dichlorobenzene from house crickets, which was identified with a library match of ∼90%.

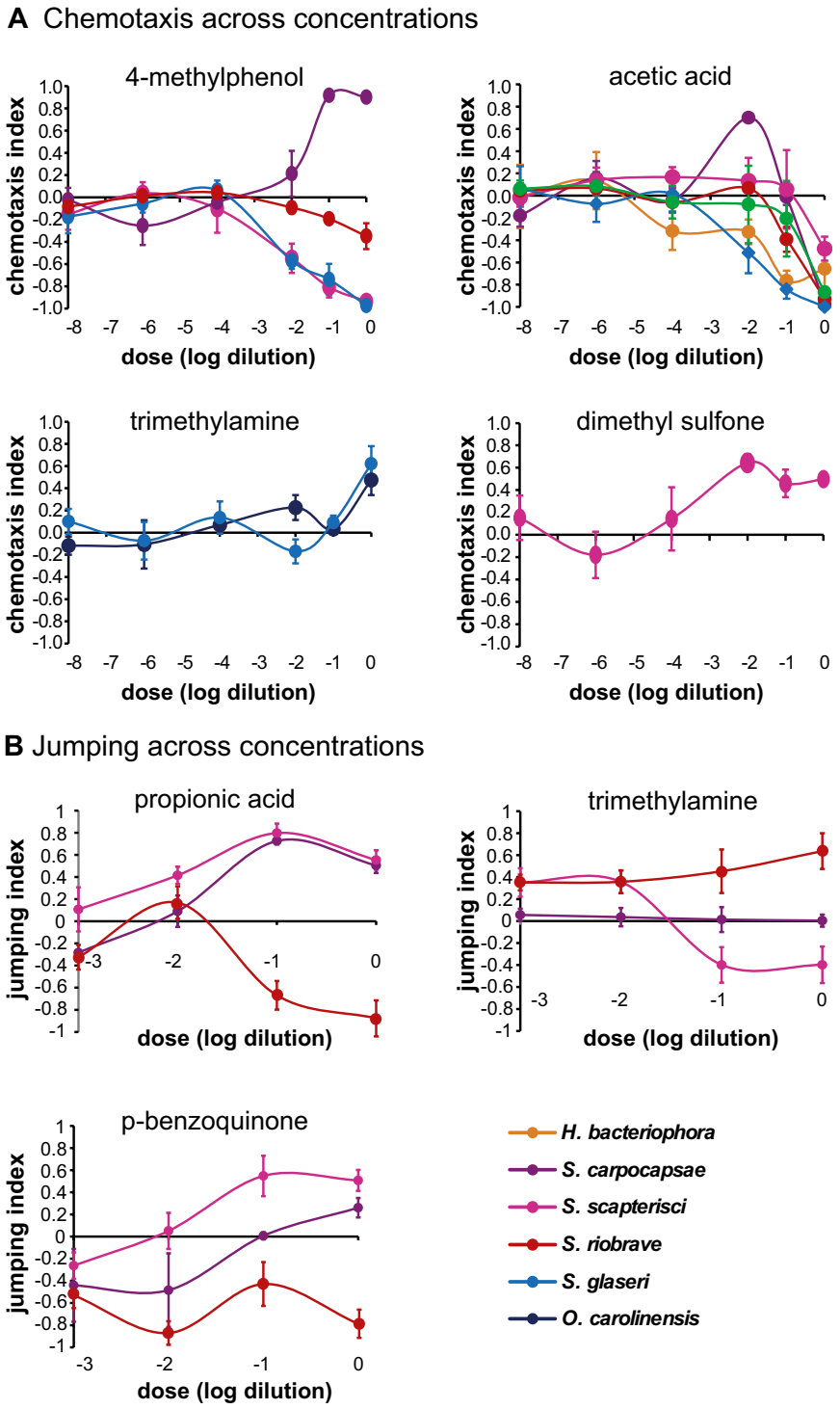

Fig. S5. Dose–response analysis for selected host-derived odorants. (*A*) Chemotaxis behavior across concentrations. *n* = 4–8 trials for each EPN–odorant combination. Mean, *n*, and SEM values for each assay are given in Dataset S13. (*B*) Jumping behavior across concentrations. *n* = 2 trials for each EPN–odorant combination. Mean, *n*, and SEM values for each assay are given in Dataset S14.

Dataset S1. EPN responses to live potential hosts

Dataset S1

Shown are mean values for the C.I. and J.I. of each EPN species in response to each potential invertebrate host in the presence and absence of soda lime to remove CO_2 chemically. The number of trials (n) and SEM are shown also. Missing values indicate EPN–host combinations that were not tested with soda lime because no attraction was observed in the no-soda-lime condition. Data are from Figs. 1 and 4*A*.

Dataset S2. Results of statistical analysis comparing the responses of the different EPNs in a chemotaxis assay

Dataset S2

P values were determined using a two-factor ANOVA with replication with a Bonferroni posttest. Data are from Fig. 1*B*; ns, not significant ($P > 0.05$).

Dataset S3. Results of statistical analysis comparing the responses elicited by the different potential hosts in a chemotaxis assay

Dataset S3

P values were determined using a two-factor ANOVA with replication with a Bonferroni posttest. Data are from Fig. 1*B*; ns, not significant ($P > 0.05$).

Dataset S4. Results of statistical analysis comparing the responses of the different EPNs in a jumping assay

Dataset S4

P values were determined using a two-factor ANOVA with replication with a Bonferroni posttest. Data are from Fig. 1*D*; ns, not significant ($P > 0.05$).

Dataset S5. Results of statistical analysis comparing the responses elicited by the different potential hosts in a jumping assay

Dataset S5

P values were determined using a two-factor ANOVA with replication with a Bonferroni posttest. Data are from Fig. 1*D*; ns, not significant ($P > 0.05$).

Dataset S6. Virulence of EPNs toward potential hosts

Dataset S6

Shown are mean values for death, growth, reproduction, and emergence for each EPN–host combination. Data are from Fig. 2.

Dataset S7. EPN responses to CO_2

Dataset S7

Shown are mean values for the C.I. and J.I. of each EPN species in response to different concentrations of CO_2 in a standard chemotaxis assay and a competition chemotaxis assay. The number of trials (*n*) and SEM are shown also. Data are from Fig. 3.

Dataset S8. Results of statistical analysis comparing the responses of each EPN to potential hosts in the presence and absence of CO_2 in a chemotaxis assay

Dataset S8

P values were determined using a two-factor ANOVA with replication with a Bonferroni posttest. Data are from Figs. 1*B* and 4*A*.

Dataset S9. Results of statistical analysis comparing the responses of each EPN to potential hosts in the presence and absence of CO_2 in a jumping assay

Dataset S9

P values were determined using a two-factor ANOVA with replication with a Bonferroni posttest. Data are from Figs. 1*D* and 4*A*.

Dataset S10. EPN responses to host-derived odorants

Dataset S10

Shown are mean values for the C.I. and J.I. of each EPN species in response to a panel of host-derived odorants. The number of trials (*n*) and SEM are shown also. Data are from Figs. 6 and 7.

Dataset S11. Results of statistical analysis comparing the responses of the different EPNs to host-derived odorants in a chemotaxis assay

Dataset S11

P values were determined using a two-factor ANOVA with replication with a Bonferroni posttest. Data are from Fig. 6*A*.

Dataset S12. Results of statistical analysis comparing the responses of the different EPNs to host-derived odorants in a jumping assay

Dataset S12

P values were determined using a two-factor ANOVA with replication with a Bonferroni posttest. Data are from Fig. 6*B*.

Dataset S13. Dose–response analysis for selected host-derived odorants in a chemotaxis assay

Dataset S13

Shown are mean values for the C.I. of EPNs to selected host-derived odorants across concentrations. The number of trials (*n*) and SEM are shown also. Data are from Fig. S5*A*.

Dataset S14. Dose–response analysis for selected host-derived odorants in a jumping assay

Dataset S14

Shown are mean values for the J.I. of EPNs to selected host-derived odorants across concentrations. The number of trials (*n*) and SEM are shown also. Data are from Fig. S5*B*.